Linear-Chain Structures of Platinum(II) Diimine Complexes

William B. Connick, Richard E. Marsh, William P. Schaefer, and Harry B. Gray*

Beckman Institute, California Institute of Technology, Pasadena, California 91125

The structures of three linear-chain platinum(II) diimine complexes have been determined [Pt···Pt, Å]: Pt(bpm)-Cl$_2$·0.5(nmp) (**3**) [3.411(1), 3.371(1)], Pt(phen)(CN)$_2$ (**6**) [3.338(1), 3.332(1)], and Pt(bpy)(NCS)$_2$ (**7**) [3.299(2)] (bpm = 2,2′-bipyrimidine, phen = 1,10-phenanthroline, bpy = 2,2′-bipyridine, nmp = 1-methyl-2-pyrrolidinone). The Pt···Pt distances in these and in seven related compounds range from 3.24 to 3.49 Å. While we find evidence of interligand interactions influencing these structures, the Pt···Pt bonds are the most important of the stacking forces. The metal−metal distances are generally consistent with an electronic structural model in which σ-donor/π-acceptor ligands strengthen Pt···Pt bonding interactions (for example, the Pt···Pt distances in **3** are 0.04 and 0.08 Å shorter than in the bpy analogue). We have also found that the yellow form of Pt(dmbpy)(NCO)$_2$ (**1b**) (4,4′-dimethyl-2,2′-bipyridine) has a columnar structure; however, in contrast to the linear-chain form (**1**), which is orange, the Pt atoms are well separated (>4.9 Å). Interestingly, the yellow form is 7% denser than the orange form; this result is consistent with the concept that directed intermolecular interactions give rise to lower density polymorphs. Crystal data: (**3**) monoclinic, *C2/m* (No. 12), *a* = 12.668(4) Å, *b* = 15.618(6) Å, *c* = 6.704(3) Å, β = 93.43(3)°, *Z* = 4; (**6**) orthorhombic, *Pbca* (No. 61), *a* = 38.731(13) Å, *b* = 18.569(3) Å, *c* = 6.628(1) Å, *Z* = 16; (**7**) orthorhombic, *Pbcm* (No. 57), *a* = 10.349(3) Å, *b* = 19.927(5) Å, *c* = 6.572(3) Å, *Z* = 4; (**1b**) monoclinic, *C2/c* (No. 15), *a* = 17.313(4) Å, *b* = 12.263(3) Å, *c* = 14.291(4) Å, β = 114.00(2)°, *Z* = 8.

Introduction

Square planar platinum(II) complexes often form linear-chain materials with striking spectroscopic properties. In these structures, the planar molecules stack with short Pt···Pt contacts (<3.5 Å), and the Pt···Pt···Pt chain is sometimes slightly zigzag:[1]
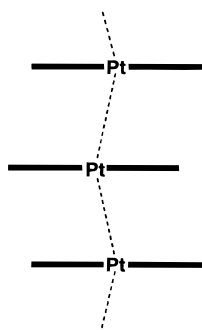
In analogy to hydrogen bonds,[2] this weak bonding interaction between d[8] metal centers is a potentially useful tool for the controlled assembly of molecules. Here we examine the factors governing the stacking of platinum(II) diimine complexes.

The stabilization of these structures is attributable in part to bonding interactions arising from the overlap of the 5d$_{z^2}$ and 6p$_z$ orbitals of adjacent metal centers:
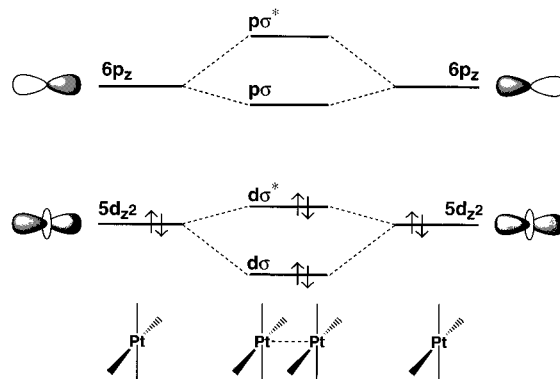
The fully occupied 5d$_{z^2}$ levels of adjacent platinum centers split to give bonding (dσ) and antibonding (dσ*) molecular orbitals; similarly, the unoccupied 6p$_z$ levels split to give pσ and pσ* orbitals. Since both the dσ* and dσ levels are fully occupied, no formal Pt−Pt bonding occurs. However, configuration interaction with the pσ and pσ* orbitals stabilizes the dσ* and dσ levels, resulting in net favorable interactions.[3] This description accounts for the solution and solid-state stability, as well as the photophysical properties, of a wide range of stacked complexes with d[8] metal centers, including those of Rh(I), Ir(I), and Pt(II).[1]

Because the metal−metal interactions in these systems are relatively weak, the resulting metal−metal distance is often strongly dependent on other factors as well. For example, the metal−metal distance in linear-chain tetracyanoplatinate salts varies from 3.7 to 3.1 Å, depending on the cation and the water content.[4] Similarly, electrostatic interactions such as in [Pt(NH$_3$)$_4$][PtCl$_4$] (Magnus' green salt),[5] as well as steric effects, strongly influence the stacking of complexes. Thus, the stacked

---

[⊗] Abstract published in *Advance ACS Abstracts,* January 1, 1997.
(1) *Extended Linear Chain Compounds*; Miller, J. S., Ed.; Plenum Press: New York, 1982; Vols. 1−3.

neutral platinum(II) diimine complexes, which are relatively free of hydrogen bonds and have comparable steric properties, are well suited for investigations of Pt···Pt interactions in the absence of other strong intermolecular forces.

Since the original work on Pt(bpy)Cl$_2$ (bpy = 2,2′-bipyridine) by Osborn and Rogers,[6] only a few linear-chain platinum(II) diimine complexes have been structurally characterized.[7−13] Obtaining suitable crystals for X-ray diffraction studies is generally difficult, in part due to poor solubility. Moreover, since growth is rapid along the chain axis, crystals are typically thin needles and frequently twinned. Here we report the structures of three linear-chain materials, as well as the structure of the yellow form of Pt(dmbpy)(NCO)$_2$ (dmbpy = 4,4′-dimethyl-2,2′-bipyridine), which in contrast to its orange form,[10,11] has no short Pt···Pt contacts (<4 Å). Our examination of these structures and those of related compounds suggests that the electronic properties of the ligands influence the Pt···Pt interactions.

Experimental Section

Crystal Preparation. Pt(bpm)Cl$_2$,[14] Pt(phen)(CN)$_2$,[7] Pt(bpy)-(NCS)$_2$,[15] and Pt(dmbpy)(NCO)$_2$[10] (bpm = 2,2′-bipyrimidine, phen = 1,10-phenanthroline) were prepared according to published protocols. Needle-shaped crystals of Pt(bpm)Cl$_2$·0.5 nmp (**3**) (nmp = 1-methyl-2-pyrrolidinone) were grown by slow evaporation of a solution of nmp. Thin, needle-shaped crystals of Pt(phen)(CN)$_2$ (**6**) were prepared by slow cooling of a hot dimethyl sulfoxide solution seeded with crystals from an earlier trial. Also, bladelike crystals of Pt(bpy)(NCS)$_2$ (**7**) were grown by vapor diffusion of Et$_2$O into a dmf (*N,N*-dimethylformamide) solution. Orange needles (**1**) and yellow rectangular prisms (**1b**) of Pt(bpy)(NCO)$_2$ were prepared in roughly equal amounts by slow evaporation of an nmp solution. The two polymorphs were separated

(2) For examples of hydrogen-bonded supramolecular structures, see: Aoyama, Y.; Endo, K.; Anzai, T.; Yamaguchi, Y.; Sawaki, T.; Kobayashi, K.; Kanehisa, N.; Hashimoto, H.; Kai, Y.; Masuda, H. *J. Am. Chem. Soc.* **1996**, *118*, 5562. Reddy, D. S.; Ovchinnikov, Y. E.; Shishkin, O. V.; Struchkov, Y. T.; Desiraju, G. R. *J. Am. Chem. Soc.* **1996**, *118*, 4085. Schwiebert, K. E.; Chin, D. N.; MacDonald, J. C.; Whitesides, G. M. *J. Am. Chem. Soc.* **1996**, *118*, 4018. Munakata, M.; Wu, L. P.; Yamamoto, M.; Kuroda-Sowa, T.; Maekawa, M. *J. Am Chem. Soc.* **1996**, *118*, 3117. Marsh, A.; Silvestri, M.; Lehn, J.-M. *J. Chem. Soc., Chem. Commun.* **1996**, 1527. Abrahams, B. F.; Egan, S. J.; Hoskins, B. F.; Robson, R. *J. Chem. Soc., Chem. Commun.* **1996**, 1099; Aakeröy, C. B.; Nieuwnhuyzen, M. *J. Mol. Struct.* **1996**, *374*, 223. Videnovaadrabinska, V. *J. Mol. Struct.* **1996**, *374*, 199. Desiraju, G. R. *Angew. Chem., Int. Ed. Engl.* **1995**, *34*, 2311. Videnovaadrabinska, V.; Etter, M. C. *J. Chem. Crystallogr.* **1995**, *25*, 823. Burrows, A. D.; Chan, C.-W.; Chowdhry, M. M.; McGrady, J. E.; Mingos, D. M. P. *Chem. Soc. Rev.* **1995**, *24*, 329. Wang, X.; Simard, M.; Wuest, J. D. *J. Am. Chem. Soc.* **1994**, *116*, 12119. Zerkowski, J. A.; Mathias, J. P.; Whitesides, G. M. *J. Am. Chem. Soc.* **1994**, *116*, 4305. Subramanian, S.; Zaworotko, M. J. *Coord. Chem. Rev.* **1994**, *137*, 357. MacDonald, J. C.; Whitesides, G. M. *Chem. Rev.* **1994**, *94*, 2383. Aakeröy, C. B.; Seddon, K. R. *Chem. Soc. Rev.* **1993**, *22*, 397. Etter, M. C. *J. Phys. Chem.* **1991**, *95*, 4601; Lehn, J.-M. *Angew. Chem., Int. Ed. Engl.* **1990**, *29*, 1304.
(3) Krogmann, K. *Angew. Chem., Int. Ed. Engl.* **1969**, *8*, 35.
(4) Gliemann, G.; Yersin, H. *Struct. Bonding* **1985**, *62*, 87.
(5) Atoji, M.; Richardson, J. W.; Rundle, R. E. *J. Am. Chem. Soc.* **1957**, *79*, 3017.
(6) Osborn, R. J.; Rogers, D. *J. Chem. Soc., Dalton Trans.* **1974**, 1002.
(7) Che, C.-M.; He, L.-Y.; Poon, C.-K.; Mak, T. C. M. *Inorg. Chem.* **1989**, *28*, 3081.
(8) Coyer, M. J.; Herber, R. H.; Cohen, S. *Inorg. Chim. Acta* **1990**, *175*, 47.
(9) Biedermann, J.; Gliemann, G.; Klement, U.; Range, K.-J.; Zabel, M. *Inorg. Chim. Acta* **1990**, *171*, 35.
(10) Coyer, M. J.; Herber, R. H.; Cohen, S. *Acta Crystallogr.* **1991**, *C47*, 1376.
(11) Marsh, R. E. *Acta Crystallogr.* **1994**, *A50*, 450.
(12) Kato, M.; Sasano, K.; Kosuge, C.; Yamazaki, M.; Yano, S.; Kimura, M. *Inorg. Chem.* **1996**, *35*, 116.
(13) Connick, W. B.; Henling, L. M.; Marsh, R. E. *Acta Crystallogr.* **1996**, *B52*, 817.
(14) Kiernan, P. M.; Ludi, A. *J. Chem. Soc., Dalton Trans.* **1978**, 1127.
(15) Coyer, M. J.; Croft, M.; Chen, J.; Herber, R. H. *Inorg. Chem.* **1992**, *31*, 1752.

Table 1. Crystallographic Data for Pt(bpm)Cl$_2$·0.5nmp (**3**), Pt(phen)(CN)$_2$ (**6**), Pt(bpy)(NCS)$_2$ (**7**), and Pt(dmbpy)(NCO)$_2$ (**1b**)

3	PtC$_8$H$_6$N$_4$Cl$_2$·0.5(C$_5$H$_9$NO)	fw = 473.72
	a = 12.668(4) Å	space group: *C2/m* (No. 12)
	b = 15.618(6) Å	ρ_{calc} = 2.38 g/cm^3
	c = 6.704(3) Å	μ = 112.1 cm^{-1} (θ_{max} = 25°)
	β = 93.43(3)°	978 indep reflcns ($\pm h, \pm k, l$)
	V = 1324.0(8) Å^3	R^a = 0.038 ($R_w{}^b$ = 0.069)
	Z = 4	GOF^c = 1.55 (83 params)
6	PtC$_{14}$H$_8$N$_4$	fw = 427.32
	a = 38.731(13) Å	space group: *Pbca* (no. 61)
	b = 18.569(3) Å	ρ_{calc} = 2.38 g/cm^3
	c = 6.628(1) Å	μ = 118.9 cm^{-1} (θ_{max} = 20°)
	V = 4766(2) Å^3	2213 indep reflcns ($\pm h, \pm k, l$)
	Z = 16	R^a = 0.069 ($R_w{}^b$ = 0.086)
		GOF^c = 1.61 (164 params)
7	PtC$_{12}$H$_8$N$_4$S$_2$	fw = 467.43
	a = 10.349(3) Å	space group: *Pbcm* (no. 57)
	b = 19.927(5) Å	ρ_{calc} = 2.29 g/cm^3
	c = 6.572(3) Å	μ = 107.4 cm^{-1} (θ_{max} = 20°)
	V = 1355.3(7) Å^3	710 indep reflcns ($h, k, \pm l$)
	Z = 4	R^a = 0.050 ($R_w{}^b$ = 0.099)
		GOF^c = 2.80 (67 param)
1b	PtC$_{14}$H$_{12}$N$_4$O$_2$	fw = 463.36
	a = 17.313(4) Å	space group: *C2/c* (no. 15)
	b = 12.263(3) Å	ρ_{calc} = 2.22 g/cm^3
	c = 14.291(4) Å	μ = 102.4 cm^{-1} (θ_{max} = 25°)
	β = 114.00(2)°	2016 ind reflcns ($\pm h, \pm k, l$)
	V = 2771.8(11) Å^3	R^a = 0.031 ($R_w{}^b$ = 0.048)
	Z = 8	GOF^c = 1.24 (191 params)

^{a} $R = \sum|F_o - |F_c||/\sum|F_o|$. ^{b} $R_w = (\sum w(F_o^2 - F_c^2)^2/\sum w(F_o^2)^2)^{1/2}$. ^{c} GOF = $(\sum w(F_o^2 - F_c^2)^2/(n - p))^{1/2}$, where n is the number of data and p is the number of parameters refined.

using a dissecting needle and microscope with visible or UV illumination of the sample; the yellow crystals (**1b**) are weakly luminescent (green) at room temperature, whereas the orange crystals (**1**) exhibit an intense orange luminescence.

X-ray Crystallography. Diffraction data were collected at room temperature (294 K) on an Enraf-Nonius CAD4 diffractometer (Mo Kα radiation and graphite monochromator, λ = 0.710 73 Å). Intensities were corrected for Lorentz and polarization effects; data for **1b** and **6** were corrected for absorption (Ψ scans of six reflections). The intensities of three standard reflections showed no variations greater than those predicted by counting statistics. The Pt coordinates were obtained from Patterson maps, and remaining non-hydrogen atom positions were determined from successive structure factor, Fourier calculations. Ligand H atoms were positioned by calculation (C−H, 0.95 Å) and were assigned isotropic *B*'s approximately 1.1 times those of the attached carbon atoms. Weights were taken as $1/\sigma^2(F_o^2)$; variances $[\sigma^2(F_o^2)]$ were derived from counting statistics plus an additional term, $(0.014F_o^2)^2$; variances of the merged data were determined by propagation of esd's plus another additional term, $(0.014-\langle F_o^2 \rangle)^2$. Atomic scattering factors were taken from Cromer and Waber.[16,17] Computer programs used were those of the CRYM crystallographic computing system[18] and ORTEP.[19] Pertinent data are collected in Table 1.

Pt(bpm)Cl$_2$·0.5nmp (3). Diffractometer data and Weissenberg photographs indicated that the monoclinic crystal was twinned across the (001) plane; reflections of the type *hk*0 appeared normal, while those with *l* ≠ 0 were split. Because β is so close to 90°, the reflections with *l* = 1 were insufficiently separated to be measured independently, and these data were discarded. From the photographs, the two twins were estimated to be equal in size, and the intensities of the *hk*0

(16) Cromer, D. T.; Waber, J. T. In *International Tables For X-ray Crystallography*; Kynoch Press: Birmingham, England, 1974; Vol. IV, pp 99−101.
(17) Cromer, D. T. In *International Tables For X-ray Crystallography*; Kynoch Press: England, Birmingham, 1974; Vol. IV, pp 149−151.
(18) Duchamp, D. J. *American Crystallographic Association Meeting*; Bozeman, Montana, 1964; Paper B14, pp 29−30.
(19) Johnson, C. K. ORTEPII. Report ORNL-5138; Oak Ridge National Laboratory: Oak Ridge, TN, 1976.

reflections were halved. The reflections collected for absorption correction were also contaminated by the twinning; loss of the crystal during the January 17, 1994, Northridge earthquake precluded further measurements.

The solvent occupies a region with $2/m$ symmetry; thus, each region has four orientations of an nmp molecule. The positions of the solvent atoms were taken from a difference Fourier map. Several atoms were sufficiently isolated to allow refinement. A difference map in the plane of the solvent at the end of the refinement showed peaks of 1 e $\mathring{A}^{-3}$ near the N atom positions, but no other peaks so large. Though the C—O distance (1.25(2) $\mathring{A}$) is reasonable, the B value of the oxygen atoms refined to 0.3(3), an unrealistically small number. We can find no chemical or crystallographic reason for this small value. No reasonable solvent combination could be found to account for the analysis of the bulk material. Anal. Calcd for $C_{10.5}Cl_2H_{10.5}N_{4.5}O_{0.5}Pt$: C, 26.62; H, 2.23; N, 13.31; O, 1.69; Cl, 14.97. Found: C, 26.24; H, 1.93; N, 13.07; O, 3.99; Cl, 17.21. However, elemental analysis of the dried solid was entirely consistent with $Pt(bpm)Cl_2$. Anal. Calcd for $C_8Cl_2H_6N_4Pt$: C, 22.65; H, 1.43; N, 13.21. Found: C, 22.61; H, 1.50; N, 13.20.

Pt(phen)(CN)$_2$ (6). In addition to the systematic absences characteristic of *Pbca*, the diffraction data exhibit a curious pattern of reflections with $h \neq 4n$ having weak intensity. This observation and the presence of a strong peak in the Patterson map indicate that the Pt atoms are separated by $a/4$. Judicious positioning of the Pt atoms followed by a structure factor and a Fourier map calculation gave the positions of the remaining non-hydrogen atoms. The two molecules in the asymmetric unit are *almost* related by a translation of $^1/_4$ along x. This pseudosymmetry results in strong correlation between parameters of atoms in the two molecules (*e.g.*, correlation coefficients of Pt1, Pt2, $x = -0.45$, $y = -0.67$, $z = -0.23$; N1, N5, $x = -0.71$, $y = -0.68$, $z = -0.15$). As a result, several atoms could not be refined anisotropically, and all C and N atoms were refined isotropically.

Pt(bpy)(NCS)$_2$ (7). The crystal was small and diffracted poorly; only the Pt and S atoms were refined anisotropically.

Pt(dmbpy)(NCO)$_2$ (1b). A difference map showed that the methyl H atoms are disordered; these atoms were modeled in two orientations in a staggered arrangement. The cyanate ligands were modeled as N-bonded to the Pt. Refinement of the structure with O-bonded cyanate groups gave R (0.0338), $R_{3\sigma}$ (0.0244), and S (1.40) values significantly greater than those resulting from refinement of the N-bonded structure; moreover, refinement of the structure with a mixture of N- and O-bonded cyanate also indicated N-bonded coordination [96(5)% Pt—N1—C1—O1; 88(6)% Pt—N2—C2—O2].

Results

Selected distances and angles for **1b**, **3**, **6**, and **7** are given in Table 2. Figure 1 shows the platinum complexes and Figure 2 shows views of their packing.

Pt(bpm)Cl$_2$·0.5nmp (3). Kiernan and Ludi[14] previously noted that $Pt(bpm)Cl_2$ forms both yellow and red solids; the color of the red material is suggestive of a linear-chain structure. The approximately planar $Pt(bpm)Cl_2$ units are bisected by a mirror plane ($y = 0$) passing through the Pt atom. Overall, the molecular geometry is similar to that found for $Pt(bpy)Cl_2$.[6,20−23] The Pt—N and Pt—Cl distances (2.006(8), 2.294(3) $\mathring{A}$) and the diimine bite and Cl—Pt—Cl angles are nearly identical with the values reported for the red and yellow forms of $Pt(bpy)Cl_2$ (yellow form, 2.006(10) and 2.011(10) $\mathring{A}$, 2.281(4) and 2.300(3) $\mathring{A}$, and 80.6(4) and 89.1(1)°;[21,22] red form, 2.009(6) and 2.302(2) $\mathring{A}$ and 80.2(2) and 89.1(1)°).[23] There are no unusually close contacts between the disordered solvent region and the Pt complex.

The complexes stack along the c axis to form a chain of Pt-

(20) Textor, V. M.; Oswald, H. R. *Z. Anorg. Allg. Chem.* **1974**, *407*, 244.
(21) Canty, A. J.; Skelton, B. W.; Traill, P. R.; White, A. H. *Aust. J. Chem.* **1992**, *45*, 417.
(22) Herber, R. H.; Croft, M.; Coyer, M. J.; Bilash, B.; Sahiner, A. *Inorg. Chem.* **1994**, *33*, 2422.
(23) Connick, W. B.; Henling, L. M.; Marsh, R. E.; Gray, H. B. *Inorg. Chem.* **1996**, *35*, 6261.

Table 2. Selected Bond Lengths ($\mathring{A}$) and Angles (deg) for **3**, **6**, **7**, and **1b**[a]

Compound **3**			
Pt—N1	2.006(8)	N1—Pt—Cl	95.2(2)
Pt—Cl	2.294(3)	N1—Pt—N1′	80.0(3)
N1—C1	1.339(12)	N1—Pt—Cl′	175.2(2)
C1—C1′	1.463(13)	Cl—Pt—Cl′	89.6(1)
Compound **6**			
Pt1—N1	2.08(2)	N1—Pt1—C13	93.8(11)
Pt1—N2	2.06(2)	N1—Pt1—N2	81.2(8)
Pt1—C13	1.95(3)	N1—Pt1—C14	175.8(10)
Pt1—C14	1.94(3)	C13—Pt1—C14	90.2(12)
C13—N3	1.16(4)	N2—Pt1—C13	175.0(10)
C14—N4	1.17(4)	N2—Pt1—C14	94.8(10)
N1—C5	1.39(4)	Pt1—C13—N3	178.5(3)
N2—C6	1.39(3)	Pt1—C14—N4	175.8(3)
Pt2—N5	2.04(2)	N5—Pt2—C27	96.2(12)
Pt2—N6	1.99(2)	N5—Pt2—N6	79.7(8)
Pt2—C27	1.89(3)	N5—Pt2—C28	175.3(11)
Pt2—C28	1.93(3)	C27—Pt2—C28	88.5(13)
C27—N7	1.17(5)	N6—Pt2—C27	175.8(11)
C28—N8	1.16(4)	N6—Pt2—C28	95.7(10)
N5—C19	1.38(4)	Pt2—C27—N7	176.4(3)
N6—C20	1.38(3)	Pt2—C28—N8	174.1(3)
Compound **7**			
Pt—N3	2.06(2)	N1—Pt—N3	93.5(8)
Pt—N4	1.91(2)	N3—Pt—N4	83.1(8)
Pt—N1	1.94(2)	N2—Pt—N3	177.4(9)
Pt—N2	2.11(3)	N1—Pt—N2	89.1(9)
N1—C1	1.11(3)	N1—Pt—N4	176.6(8)
N2—C2	1.05(4)	N2—Pt—N4	94.3(9)
C1—S1	1.68(3)	Pt—N1—C1	174(2)
C2—S2	1.57(3)	Pt—N2—C2	169(3)
Compound **1b**			
Pt—N3	2.005(5)	N1—Pt—N3	94.6(2)
Pt—N4	2.001(5)	N3—Pt—N4	81.2(2)
Pt—N1	1.985(6)	N2—Pt—N3	175.4(2)
Pt—N2	2.007(6)	N1—Pt—N2	89.9(2)
N1—C1	1.141(9)	N1—Pt—N4	175.4(2)
N2—C2	1.136(9)	N2—Pt—N4	94.4(2)
C1—O1	1.203(9)	Pt—N1—C1	160.2(6)
C2—O2	1.194(9)	Pt—N2—C2	153.9(6)
N3—C8	1.373(7)	N1—C1—O1	176.9(8)
N4—C9	1.373(7)	N2—C2—O2	176.9(8)

[a] Primed atoms are related by a mirror plane: x, $-y$, z.

(bpm)Cl$_2$ units with short interplanar spacings (3.3−3.4 $\mathring{A}$); successive molecules are related by an inversion center, and thus appear rotated by 180° in an antiparallel arrangement when viewed along the c axis (Figure 3). This packing leaves channels between the chains that are occupied by solvent. The mean plane defined by the Pt and coordinated N and Cl atoms is nearly perpendicular to the stacking axis; the angle is 86.1(1)°. The Pt atoms are offset from the chain axis by 0.257(1) $\mathring{A}$ along a, but lie very close to $z = ^1/_4$ and $^3/_4$; the two Pt···Pt distances (3.371(1), 3.411(1) $\mathring{A}$) along the chain are nearly equal with a Pt···Pt···Pt angle of 162.55(2)°. The distances are slightly shorter than that found for stacked $Pt(bpy)Cl_2$ complexes (3.449(1) $\mathring{A}$; Pt···Pt···Pt, 161.03(3)°).[6,23]

Pt(phen)(CN)$_2$ (6). The violet color of this material[7] prompted our structural investigation. Two $Pt(phen)(CN)_2$ molecules, approximately related by a translation of 1/4 along a, form the asymmetric unit (Figure 1bc). During refinement, this pseudosymmetry caused high correlation between the parameters describing the two molecules, and consequently the resulting distances and angles are imprecise. Taking into account the largest covariance terms, the esd of the difference (0.09 $\mathring{A}$) between the Pt1—N2 and Pt2—N6 bond lengths is 0.03 $\mathring{A}$; the esd of the difference (0.06 $\mathring{A}$) between the Pt1—C13 and Pt2—C27 bond lengths is 0.06 $\mathring{A}$.
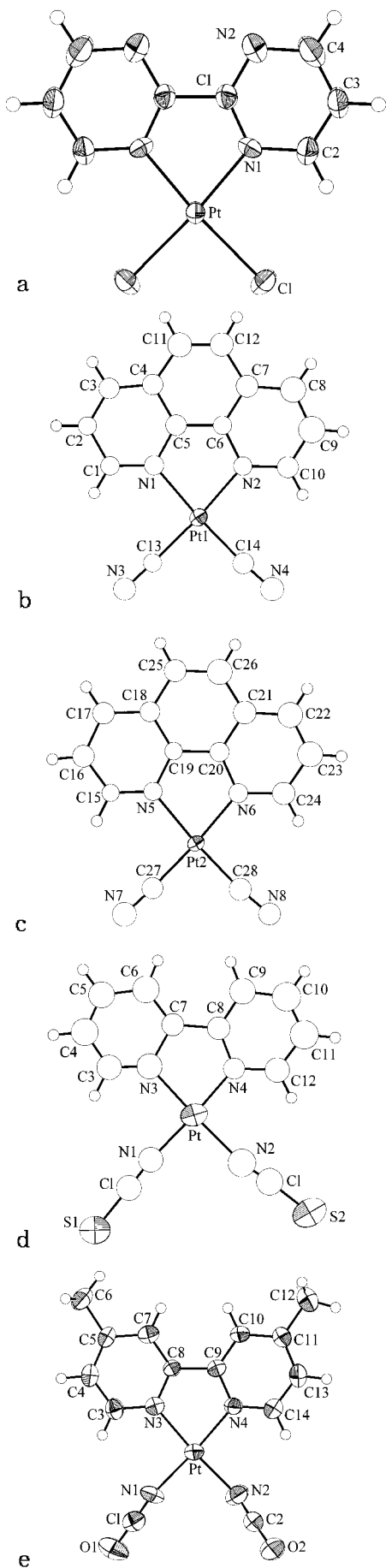
The Pt1 and Pt2 complexes stack separately along c to form two types of chains; because of the pseudosymmetry, the

a

b

c

d

e

Figure 1. ORTEP diagrams with 50% probability ellipsoids showing (a) Pt(bpm)Cl$_2$ (**3**), (b, c) both molecules of Pt(phen)(CN)$_2$ (**6**), (d) Pt(bpy)(NCS)$_2$ (**7**), and (e) Pt(dmbpy)(NCO)$_2$ (**1b**). Atoms that were refined isotropically are shown as hollow spheres; H atoms are shown as spheres of arbitrary size.

a

b

c

d
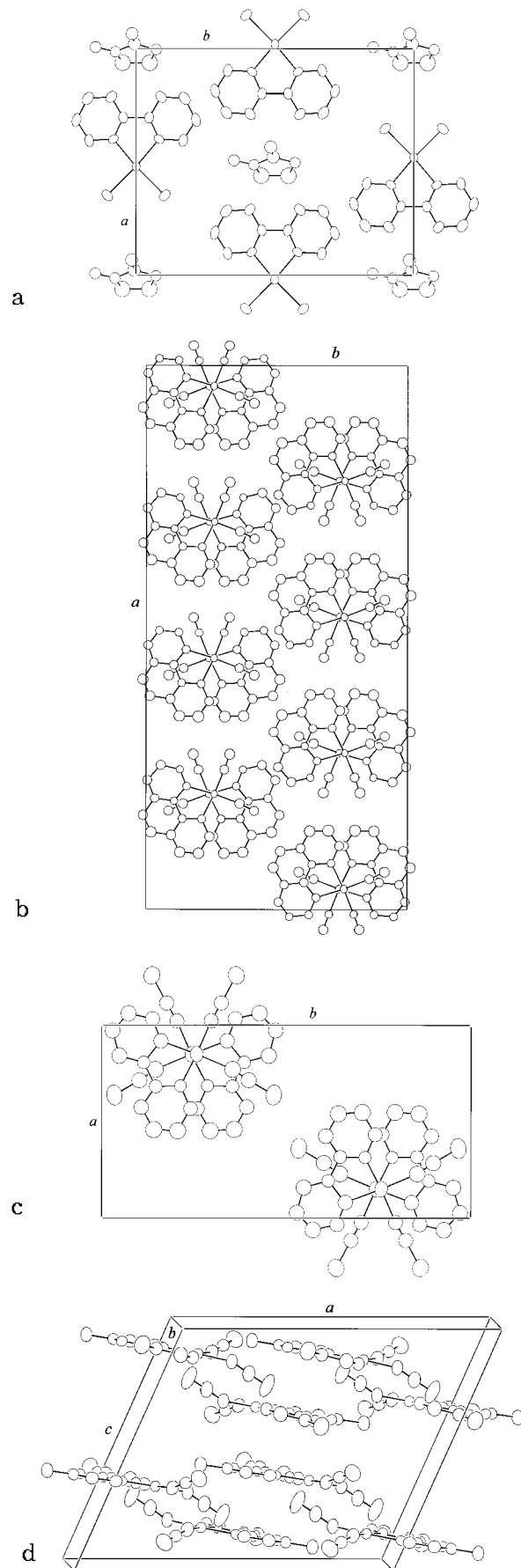
Figure 2. Crystal packing for (a) **3** (one orientation of solvent is shown and O atom has been given a *B* value of 3.3), (b) **6**, (c) **7**, and (d) **1b**. H atoms are not shown.

differences between the Pt1 and Pt2 chains are subtle. When viewed down *c*, successive units appear rotated by approxi-
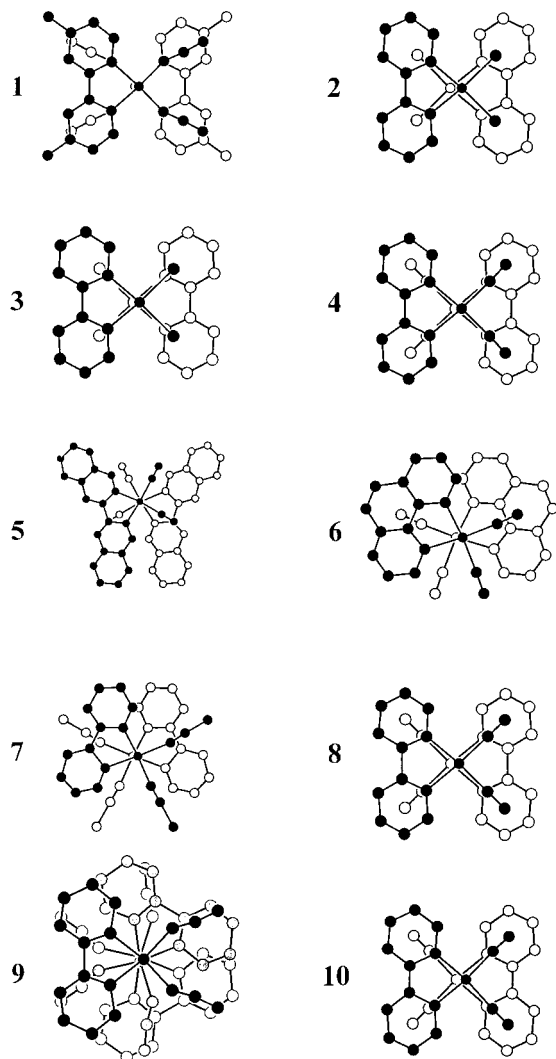
Figure 3. One repeat unit of chains **1**−**10**, viewed in projection along the stacking axis. H atoms are not shown.

mately 133° (Figure 2b); the mean plane defined by the Pt and coordinated atoms (C, N) forms an approximately 84° angle with the stacking axis. Because Pt1 and Pt2 are offset by different amounts from the chain axes (0.172(2), 0.198(2) Å), the Pt···Pt distances (3.332(1), 3.338(1) Å) and the Pt···Pt···Pt angles (168.07(4), 166.30(4)°) are slightly different for the two chains.

Pt(bpy)(NCS)₂ (7). In the solid state, the dithiocyanato complex of Pt(bpy) is known to occur in (at least) two isomeric forms, with identical stoichiometry, but distinctly different chemistry and spectroscopy. Yellow S-bonded Pt(bpy)(SCN)₂ is soluble in coordinating solvents and readily converts to the less-soluble N-bonded red form.[15,24,25] These observations led to our investigation of the structure of the red form (**7**), whose color is suggestive of Pt···Pt interactions. (We have been unable to prepare crystals of the S-bonded yellow form, apparently as a result of its tendency to convert to the red form.) The neutral Pt(bpy)(NCS)₂ units lie on mirror planes at $z = {}^1/_4$ and ${}^3/_4$; the coordination geometry of the Pt is approximately square planar. The crystal diffracted poorly and the coordinates of the lighter atoms (C and N) are not well-determined. Nevertheless, it is clear that the thiocyanate ligands are nearly linearly coordinated to the Pt with Pt−N−C(thiocyanate) angles of 176.6(8) and 177.4(9)°, characteristic of an N-bonded conformation.

The complexes stack along the *c* axis to form a chain of Pt(bpy)(NCS)₂ units with a relatively short interplanar distance of 3.286(2) Å ($=c/2$); consecutive molecules are related by the *c*-glide perpendicular to *b*. When viewed down the stacking axis (*c*), successive molecules along this chain are rotated by approximately 137°; this staggered arrangement places the bulky S atoms on the periphery of the column of molecules (Figure 2c). The Pt atoms are displaced by 0.143(2) Å (along *b*) from the chain axis, resulting in a Pt···Pt distance of 3.299(2) and a Pt···Pt···Pt angle of 170.04(5)°. Interestingly, a previous EXAFS (extended X-ray absorption fine structure) study of this material at 15 K suggested two short intermolecular Pt···Pt distances (3.24 ± 0.05 and 4.52 ± 0.02 Å).[15,26] The shorter distance is entirely consistent with our room-temperature structure; spectroscopic studies of **7** indicate a substantial contraction of the Pt···Pt separation at low temperature,[27] as often observed for Pt(II) linear chains.[4,23] The longer distance obtained from the EXAFS experiment is more difficult to explain, since the next shortest Pt···Pt distance in the crystal is 6.572(3) Å ($=c$). One explanation is that the observed peak in the radial distribution function corresponds to the *intramolecular* Pt···S distance (4.70(1), 4.72(1) Å). However, the possibility of a phase transition cannot be ruled out.

Pt(dmbpy)(NCO)₂ (1b). Slow evaporation of an nmp solution of Pt(dmbpy)(NCO)₂ gives both orange (**1**) and yellow (**1b**) crystals. The unit cell determined for a single orange crystal ($a = 18.672(8)$, $b = 11.878(5)$, $c = 6.671(5)$ Å; $\alpha = \beta = \gamma = 90°$) is in reasonable agreement with that previously reported for the linear-chain structure ($a = 18.722(6)$, $b = 11.889(5)$, $c = 6.688(5)$ Å; $\alpha = \beta = \gamma = 90°$).[10] In contrast, the yellow crystals (**1b**) contain Pt(dmbpy)(NCO)₂ units with intermolecular contacts at van der Waals distances or greater; the shortest Pt···Pt distance is 4.957(1) Å. The molecular geometry is in excellent agreement with those reported for the orange form (**1**)[11] and the unmethylated analogue, Pt(bpy)-(NCO)₂ (**9**).[8] The Pt−N−C bond angles (160.2(6) and 153.9(6)°) are significantly less than 180°, but similar to the value reported for the orange isomer (159.1(16)°).[11] A consequence of the bent cyanate coordination geometry is a substantial displacement of the C and O cyanate atoms from the Pt coordination plane (defined by Pt, N1, N2, N3, and N4): C1, −0.39; C2, 0.49; O1, −0.73; O2, 0.94 Å. In contrast, the cyanate ligands lie in the coordination plane by symmetry in the linear-chain form (**1**). The planar Pt−bipyridyl units interleave to form a columnar structure with spacings between Pt coordination planes of 3.4−3.5 Å (Figures 2e, 5a); this packing arrangement is 7% denser than that found in the orange form (**1**).[8]

Discussion

Structural Trends. Room-temperature structural data for linear-chain platinum(II) diimine complexes (**1-9**)[9,11−13,15,23] are summarized in Table 3. (The closely related compound **10**, Pt(bph)(CO)₂ (bph = biphenyl dianion),[28] also is included.) Each of the compounds **1**−**9** is intensely colored in the solid state. This color is due to an electronic transition to the ¹MLCT-[dσ*(Pt)→π*(diimine)] state, where the LUMO (π*) is predominantly centered on the diimine ligand. With decreasing

(24) Burmeister, J. L.; Basolo, F. *Inorg. Chem.* **1964**, *3*, 1587.

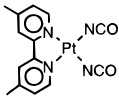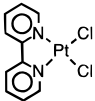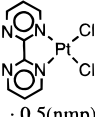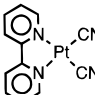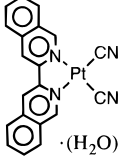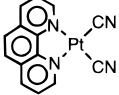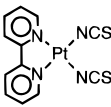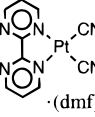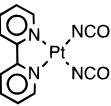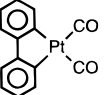(25) Kukushkin, Y. N.; Vrublevskaya, L. V.; Vlasova, R. A.; Isachkina, T. S.; Postnikova, E. S.; Sheleshkova, N. K. *Russ. J. Inorg. Chem. (Engl. Transl.)* **1985**, *30*, 224.

(26) An EXAFS study at 15 K of the yellow methylated analogue, Pt-(dmbpy)(NCS)₂, also suggested two Pt···Pt contacts: 3.63 ± 0.02 and 4.48 ± 0.05 Å (Coyer, M. J.; Herber, R. H.; Chen, J.; Croft, M.; Szu, S. P. *Inorg. Chem.* **1994**, *33*, 716).

(27) Connick, W. B.; Miskowski, V. M.; Houlding, V. H.; Gray, H. B. Manuscript in preparation.

(28) Chen, Y.-H.; Merkert, J. W.; Murtaza, Z.; Woods, C.; Rillema, D. P. *Inorg. Chim. Acta* **1995**, *240*, 41.

Table 3. Structural Properties of Linear-Chain Platinum(II) Diimines

	Compound (color) [Space group]	Pt···Pt (Å)	Interplanar Spacing (Å)	Pt···Pt···Pt (°)	Tilt Angle[a] (°)	Chain Torsion,[b] φ (°)	Pt-N(diimine) (Å)	Reference
1	Pt(dmbpy)(NCO)$_2$ (orange) [Cmcm, no. 63]	3.493(3)	3.443(3)	146.30(4)	90	180	2.01(1)	11
2	Pt(bpy)Cl$_2$ (red) [Cmcm, no. 63]	3.448(1)	3.402(1)	161.03(3)	90	180	2.009(6)	23
3	Pt(bpm)Cl$_2$·0.5(nmp) (red) [C2/m, no. 12]	3.411(1) 3.371(1)	3.330(1) 3.358(1)	162.55(2)	86.1(1)	180	2.006(8)	(d)
4	Pt(bpy)(CN)$_2$ (red) [Cmcm, no. 63]	3.346(1)	3.330(1)	169.6(1)	90	180	2.061(5)	13
5	Pt(i-biq)(CN)$_2$ (orange-red) [Pbcm, no. 57]	3.342(2)	3.341(2)	177.2	90	147	2.03(1) 2.07(1)	12
6	Pt(phen)(CN)$_2$ (violet) [Pbca, no. 61]	3.338(1) 3.332(1)	3.31^c	166.30(4) 168.07(4)	83.7(7) 83.9(7)	133	2.08(2) 2.06(2) 2.04(2) 1.99(2)	(d)
7	Pt(bpy)(NCS)$_2$ (red) [Pbcm, no. 57]	3.299(2)	3.286(2)	170.04(4)	90	137	2.06(2) 1.91(2)	(d)
8	Pt(bpm)(CN)·(dmf) (red) [Cmcm, no. 63]	3.284(1)	3.259(1)	165.9	90	180	2.042(8) 2.057(7)	9
9	Pt(bpy)(NCO)$_2$ (blue) [P3$_1$21, no. 152]	3.235(2)	3.229(2)^c	174.1	87.9	120	1.99(2)	8
10	Pt(bph)(CO)$_2$ (green) [Cmcm, no. 63]	3.2426(3)	3.2030(3)	162.1	90	180	—	28

[a] The angle between the chain axis and the mean plane defined by the Pt and the four coordinated atoms. [b] The angle of rotation of successive stacked complexes when viewed down the chain axis. [c] Average interplanar spacing. [d] This work.

Pt···Pt distance, enhanced $5d_{z^2}$···$5d_{z^2}$ interaction causes a red-shift in this transition, and the color changes from orange to blue.[29] This electronic structural model also is consistent with the yellow colors of the polymorphs of Pt(bpy)Cl$_2$ and Pt(dmbpy)(NCO)$_2$, because their shortest Pt···Pt contacts are greater than 4.4 Å.

The packing in these materials is in accord with the principle that free volume in crystals is energetically unfavorable.[30,31] The columnar structure constitutes an efficient packing motif; in fact, related compounds such as Pt(bpy)I$_2$[32] and the yellow polymorphs of **1**, **2**, and **8** (*vide infra*), which have longer Pt$\cdots$Pt contacts than their chain counterparts, also adopt columnar structures. In addition, the stacked complexes tend to avoid like−like interactions (Figure 3); when viewed down the chain axis, successive molecules are rotated by an angle, φ, ranging from 120 to 180° (Table 3). Interestingly, space group *Cmcm* (No. 63) is disproportionately represented with five of the compounds packing according to this symmetry;[33] the *mm2* site symmetry of the Pt complex in these structures readily accommodates the C_{2v} molecular symmetry, while the *c*-glide plane relating successive stacked complexes results in a φ of 180°. Thus, for compounds **1**, **2**, **4**, **8**, and **10** (as well as **3**, which crystallizes in *C2/m*), the halide or pseudohalide ligands are sandwiched between the pyridyl rings of the diimine ligands of adjacent stacked complexes (Figure 3). In analogy to Miller's description of interactions in partially oxidized Pt(oxalato) chain structures,[34] this antiparallel arrangement can accommodate weak intermolecular bonding between the occupied orbitals of the anionic ligands and the π^* orbital of the diimine ligand of an adjacent complex.

Aside from the short metal−metal contacts, several other observations point to the importance of Pt$\cdots$Pt interactions in determining the structures of these materials. Both the near-linearity of the Pt chains and the proximity of the tilt angles (the angle between the chain axis and the mean plane defined by the Pt and the four coordinated atoms) to 90° suggest a tendency to form short Pt$\cdots$Pt contacts while minimizing steric repulsions between other atoms. In addition, though the interplanar spacings of several of the compounds in Table 3 are within the range of $\pi-\pi$ stacking contacts, the diimine ligands of successive complexes are rotated away from one another. Also, when solvent is present (**3**, **5**, **8**), the solvent molecules are relegated to channels parallel to the Pt chains; these sites are disordered or partially occupied, suggesting the absence of strong specific interactions with the metal complexes. Furthermore, the Pt$\cdots$Pt distances in these complexes exhibit a characteristically strong temperature dependence. For example, cooling of **2** from room temperature to 20 K results in a 0.080(2) Å decrease in the Pt$\cdots$Pt distance;[23] similarly, at 160 K the Pt$\cdots$Pt distance in **8** is shortened by 0.024(2) Å from the room-temperature value.[35]

Interestingly, there is no definitive evidence of the Pt$\cdots$Pt interaction perturbing the molecular dimensions. However, the intramolecular electronic effects do impact on the molecular geometry. For instance, complexes with cyanide ligands generally have longer *trans* Pt−N bonds than the other complexes (*e.g.*, Pt(bpy)(CN)$_2$ (**4**), 2.061(5) Å; Pt(bpy)Cl$_2$ (**2**),

2.009(6) Å). This effect is a consequence of the strong σ-donor/π-acceptor character of the cyanide ligand.

Polymorphism. Platinum(II) diimine complexes that form linear-chain structures often exist in other crystal forms as well, indicating that the Pt$\cdots$Pt bonding may be offset by other favorable interactions.[36] For example, **4** crystallizes as a yellow hydrate, and **8** forms both yellow hydrated[37] and yellow unsolvated solids.[38] Also, as mentioned earlier, the yellow form of **7** is an S-bonded solid;[15,25] most likely, the bent thiocyanato coordination geometry[39] disfavors stacking. Furthermore, there is considerable spectroscopic evidence for monomer/chain polymorphism in several other compounds that remain structurally uncharacterized.[40]

The polymorphs of **8**[9,37,38] illustrate the interplay of subtle intermolecular forces in stabilizing these columnar structures. The hydrated form, Pt(bpm)(CN)$_2$·H$_2$O,[37] consists of a chain of dimers (Pt$\cdots$Pt = 3.44, 4.32 Å) with spacings between the molecular planes (defined by the Pt and coordinated N and C atoms) of 3.29 (intradimer) and 3.32 Å (interdimer) (Figure 4a,b). The molecules comprising the dimer adopt an antiparallel arrangement as found for the linear-chain form; the cyanide groups lie in close proximity to the bpm ligands of an adjacent molecule with a shortest C(cyanide)$\cdots$C(bpm) contact of 3.39 Å (Figure 4a). Also, there are very close contacts between the cyanide and bpm groups *between* dimers (*e.g.*, C(cyanide)$\cdots$N(bpm), 3.31; N(cyanide)$\cdots$C(bpm), 3.23 Å), once again indicating the presence of interligand bonding (Figure 4b). In the linear-chain structure (**8**),[9] the shortest C(cyanide)$\cdots$N(bpm) distance is 3.27 Å (Figure 3). Similarly, the unsolvated form consists of two chains of dimers, α (Pt$\cdots$Pt = 3.44, 4.18 Å) and β (Pt$\cdots$Pt = 3.27, 4.58 Å).[38] Interplanar spacings in the α chain are 3.26 (intradimer) and 3.25 Å (interdimer), and the stacked molecules adopt orientations remarkably similar to those of the hydrated form (Figure 4a−d). In contrast, interplanar spacings in the β chain are 3.27 and 3.49 Å, and the molecules comprising the dimer have nearly the same relative orientation (Figure 4e,f) as found for the linear-chain structure of **8** (Figure 3); the interplanar spacing in **8** is 3.26 Å with a Pt$\cdots$Pt distance of 3.28 Å. Within a dimer, the shortest C(cyanide)$\cdots$N(bpm) contact is 3.27 Å; however, the shortest contact between dimers

(29) For further discussion of the spectroscopic properties of **1**−**9**, see refs 7, 9, 23, 27, and see: Biedermann, J.; Wallfahrer, M.; Gliemann, G. *J. Lum.* **1987**, *37*, 323. Miskowski, V. M.; Houlding, V. H. *Inorg. Chem.* **1989**, *28*, 1529. Weiser-Wallfahrer, M.; Gliemann, G. *Z. Naturforsch.* **1990**, *45B*, 652. Houlding, V. H.; Miskowski, V. M. *Coord. Chem. Rev.* **1991**, *111*, 145; Miskowski, V. M.; Houlding, V. H.; Che, C.-M.; Wang, Y. *Inorg. Chem.* **1993**, *32*, 2518.
(30) Kitaigorodskii, A. I. *Organic Chemical Crystallography*; Consultants Bureau: New York, 1961.
(31) Brock, C. P.; Dunitz, J. D. *J. Am. Chem. Soc.* **1994**, *6*, 1118.
(32) Connick, W. B.; Gray, H. B. *Acta Crystallogr.* **1994**, *C50*, 1040.
(33) Biedermann et al.[9] noted that **8** also could be described in space group *Cmcm*; the quality of the data was insufficient to identify the true space group, and *P2$_1$/m* was chosen. While re-examining this structure at 160 K, we encountered similar difficulties attributable to severe twinning; our work indicates that *Cmcm* is a better choice of space group (Connick, W. B.; Henling, L. M.; Marsh, R. E. Unpublished results).
(34) Miller, J. S. *Inorg. Chem.* **1976**, *15*, 2357.

(35) In the case of **2**, the coefficient of linear thermal expansion at 300 K, α ($=(1/s)(\partial s/\partial T)$, where s is the unit-cell edge length at 300 K), along the stacking axis (9.4(3) × 10^{-5} K^{-1}) is substantially larger than the values along the axes perpendicular to this direction (1.7(1) × 10^{-5}, 1.3(1) × 10^{-5}).[23] In the case of **8**, values of α were estimated from unit cell measurements at 295[9] and 160 K,[33] assuming a linear dependence of α over this range. Along the stacking axis, α (7 × 10^{-5} K^{-1}) is greater than along one perpendicular direction (2 × 10^{-5} K^{-1}), but smaller than along the third direction (9 × 10^{-5} K^{-1}); contraction along this latter axis may reflect the ease of compression of the solvent channel.
(36) The fact that many complexes (*e.g.*, Pt(bpm)(NCO)$_2$) have not yet been shown to form linear-chain structures *is not* evidence of an intrinsically weaker Pt$\cdots$Pt electronic interaction than is present in the structures of **1**−**9**. Most likely, the propensity for a given compound to form linear chains reflects the relative stability of various packing arrangements *for that compound*; thus, the formation of stable chain structures requires sufficiently strong metal−metal interactions to offset the inefficiencies (if any) of this packing arrangement.
(37) Biedermann, J.; Gliemann, G.; Klement, U.; Range, K.-J.; Zabel, M. *Inorg. Chim. Acta* **1990**, *169*, 63.
(38) Biedermann, J.; Gliemann, G.; Klement, U.; Range, K.-J.; Zabel, M. *Inorg. Chem.* **1990**, *29*, 1884.
(39) Burmeister, J. L. *Coord. Chem. Rev.* **1990**, *105*, 77.
(40) Some examples of related compounds that exhibit polymorphism: Pt(bpm)Cl$_2$;[14] Pt(5,5′-dimethyl-bpy)(CN)$_2$ (Houlding, V. H.; Miskowski, V. M. *Coord. Chem. Rev.* **1991**, *111*, 145); Pt(bpy)(N$_3$)$_2$; Pt(bpy)(pyrazolate)Cl (Connick, W. B.; Gray, H. B. Unpublished results); and Pt(dmbpy)(ecda) (ecda = ethyl 2-cyano-3,3′-dimercaptoacrylate) (Zuleta, J. A.; Chesta, C. A.; Eisenberg, R. *J. Am. Chem. Soc.* **1989**, *111*, 8916). Crystals of the red form of Pt(dmbpy)(ecda) examined in our laboratory were badly twinned; however, diffraction photographs and diffuse reflectance measurements indicate a chain structure.
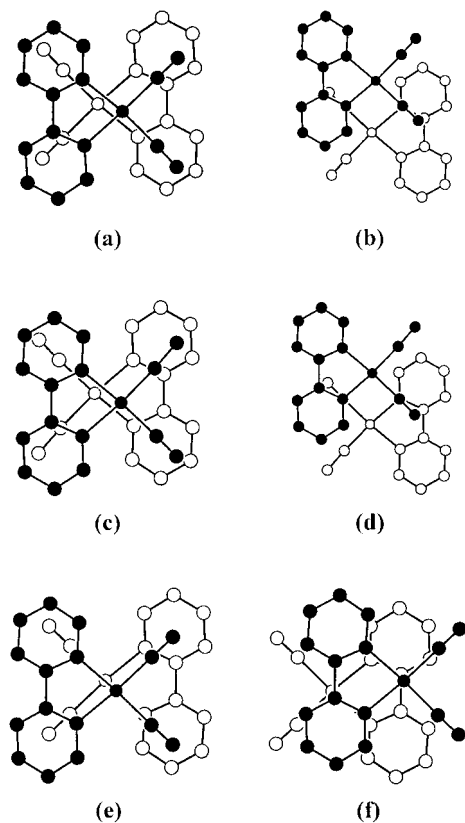
Figure 4. View in projection along the stacking axis (perpendicular to molecular planes) showing (a) intradimer and (b) interdimer interactions in $Pt(bpm)(CN)_2 \cdot H_2O$,[37] as well as (c, e) intradimer and (d, f) interdimer interactions in the α and β chains of $Pt(bpm)(CN)_2$.[38]

is 3.47 Å (Figure 4f). Thus, we find both Pt···Pt and interligand interactions in all three forms of $Pt(bpm)(CN)_2$.

The structurally characterized forms of **1** and **2** are especially interesting, since they do not involve changes in crystal composition or ligand isomerism; in both **1b** and the yellow form of $Pt(bpy)Cl_2$,[21,22] the Pt atoms are well separated (>4.4 Å). In the case of **1b**, the complexes stack to form a columnar structure with interplanar spacings of 3.44(2) and 3.46(2) Å. The planar Pt−bipyridyl units efficiently interleave to form the core of the column, whereas bending of the cyanate ligands out of the coordination plane accommodates packing of these and the methyl groups on the periphery of the column (Figure 5a). Similarly, the planar $Pt(bpy)Cl_2$ complexes in the yellow form of **2** stack in a columnar structure with an interplanar distance of 3.722(2) Å $(=c/2)$;[21] the relatively bulky Cl atoms are relegated to the periphery of the column (Figure 5b). It is intriguing that the yellow forms of **1** and **2** are, respectively, 7 and 2% *denser* than the linear-chain forms; these relative densities indicate that the linear-chain forms are *less* closely packed, consistent with the expectation that directed intermolecular interactions will give rise to lower density polymorphs. Evidently, the energy costs associated with an increase in free volume are offset by the Pt···Pt bonding interactions in the linear-chain structures.

Factors Governing Stacking. We have identified three important factors governing the stacking in this series of compounds: interligand steric repulsions, interligand charge-transfer bonding, and Pt···Pt bonding. Steric effects are suggested by the tendency of successive stacked complexes to avoid eclipsed arrangements. In addition, in the case of **1** the methyl groups account for the 0.26 Å increase in metal−metal distance with respect to **9**; again, these bulky groups are relegated to the periphery of the column of stacked molecules (Figure 3).[41] Also, it must be noted that for the series of compounds **1−10**,

complexes with chloride ligands tend to have the longest metal−metal contacts, though this observation also is consistent with electronic effects (*vide infra*). Interligand charge-transfer interactions are indicated by the antiparallel stacking motif in which the halide or pseudohalide ligands are sandwiched between neutral diimine ligands of adjacent molecules in the chain (Figure 3). From spatial overlap considerations, these interactions are expected to be weaker than those between the Pt centers. In point of fact, this type of stacking is not found in **5**, **6**, **7**, and **9**, all of which have relatively short Pt···Pt contacts. Thus, the accumulated evidence indicates that the Pt···Pt interactions are the dominant force supporting stacking.

Ligand-field strength has a primary effect on the Pt···Pt bonding, since strong-field ligands destabilize $5d_{z^2}$, enhancing the interactions of stacked complexes. The π-donor/acceptor character of the ligands has a secondary influence; π-acceptor groups decrease electron density on the metal center, thereby reducing electronic repulsions between Pt centers and favoring shorter Pt···Pt distances. Indeed, this description accounts for many empirical trends of linear-chain d^8 systems.[34,42] In the case of compounds **1−9**, the diimine ligands are good π-acceptors, and thus these molecules are well suited to form chain structures.

The Pt···Pt distances in **1−9** are in general consistent with these electronic considerations. In Table 3, there are apparent clusterings of compounds with long, medium, and short metal−metal contacts. Coordination of weak-field π-donor chloride ligands results in longer Pt···Pt distances (**2**, **3**), whereas complexes with the stronger-field N-donor ligands generally have the shortest distances (**7**, **9**). The cyanide derivatives (**4**, **5**, **6**, **8**) fall in an intermediate range.[43] The relatively long metal−metal distances in the chloride derivatives are evidently characteristic of the PtN_2Cl_2 system (Table 4). For example, *cis*-$Pt(NH_3)_2Cl_2$ complexes stack with metal distances of 3.37 and 3.41 Å;[44] in the orthorhombic form of $Pt(en)Cl_2$ (en = ethylenediamine), the Pt···Pt distance is 3.381(2) Å (*cf.*, **2** and

(41) Interestingly, though it is not certain that $Pt(dmbpy)(NCS)_2$ also forms a chain structure, an EXAFS study at 15 K suggests a Pt···Pt distance[26] that is 0.33 ± 0.02 Å longer than that found in the unmethylated analogue (**7**).

(42) For example, the series of linear-chain platinum(II) dioximates, each of which crystallizes in space group *Ibam* (No. 72), provides evidence for electronic effects on the metal−metal distance (Pt···Pt, Å): $Pt(1,2\text{-benzoquinonedioximate})_2$ (3.17); $Pt(dichloroglyoximate)_2 \cdot H_2O$ (3.18) (this compound was previously described in space group *Iba*2; however, mirror symmetry at $z = 0$ indicates that this structure would be better described in space group *Ibam*); $Pt(pyridine-2\text{-carbox-aldoximate})_2 \cdot 2H_2O$ (3.25); $Pt(dimethylglyoximate)_2$ (3.26) (Mégnamisi-Bélombé, M. *J. Solid State Chem.* **1979**, *27*, 389. Briansó, J. L.; Matheus, M. de *Afinidad* **1982**, *39*, 271; Nordquest, K. W.; Phelps, D. W.; Little, W. F.; Hodgson, D. J. *J. Am. Chem. Chem. Soc.* **1976**, *98*, 1104. Konno, M.; Okamato, T.; Shirotani, I. *Acta Crystallogr.* **1989**, *B45*, 142.) In this series, the two complexes with the shortest Pt···Pt contacts have the stronger electron-withdrawing ligands. Interestingly, the closely related linear-chain $Pt(glyoximate)_2$ complex crystallizes in $P2_1/n$ (No. 14) with a relatively long Pt···Pt distance (3.50 Å) (Ferraris, G.; Viterbo, D. *Acta Crystallogr.* **1969**, *B25*, 2066); however, the planar molecules are tilted by 72° with respect to the chain axis.

(43) We have noticed a greater tendency for platinum diimine cyanides to stack than other complexes; this trend is in accord with the strong σ-donor/π-acceptor character of the cyanide ligand. However, given these electronic considerations, it is intriguing that the cyanide derivatives (**4**, **5**, **6**, **8**) do not stack with shorter Pt···Pt distances than thiocyanate or cyanate analogues (**7**, **9**). It is unlikely that the steric demands of thiocyanate and cyanate are less than those of cyanide. Moreover, several linear-chain $Pt(CN)_4^{2-}$ salts crystallize with very short metal−metal separations (< 3.2 Å) (ref. 4; Krogmann, K.; Stephan, D. *Z. Anorg. Allg. Chem.* **1968**, *362*, 290). One explanation is that the antiparallel stacking motif of **6** and **8**, which favors interligand binding, is incompatible with the very short metal−metal separation favored by the electronic interaction of the Pt centers: thus, derivatives **5** and **6**, which do not adopt an antiparallel arrangement, favor longer separations because of the steric demands of their larger diimine ligands.

a

b
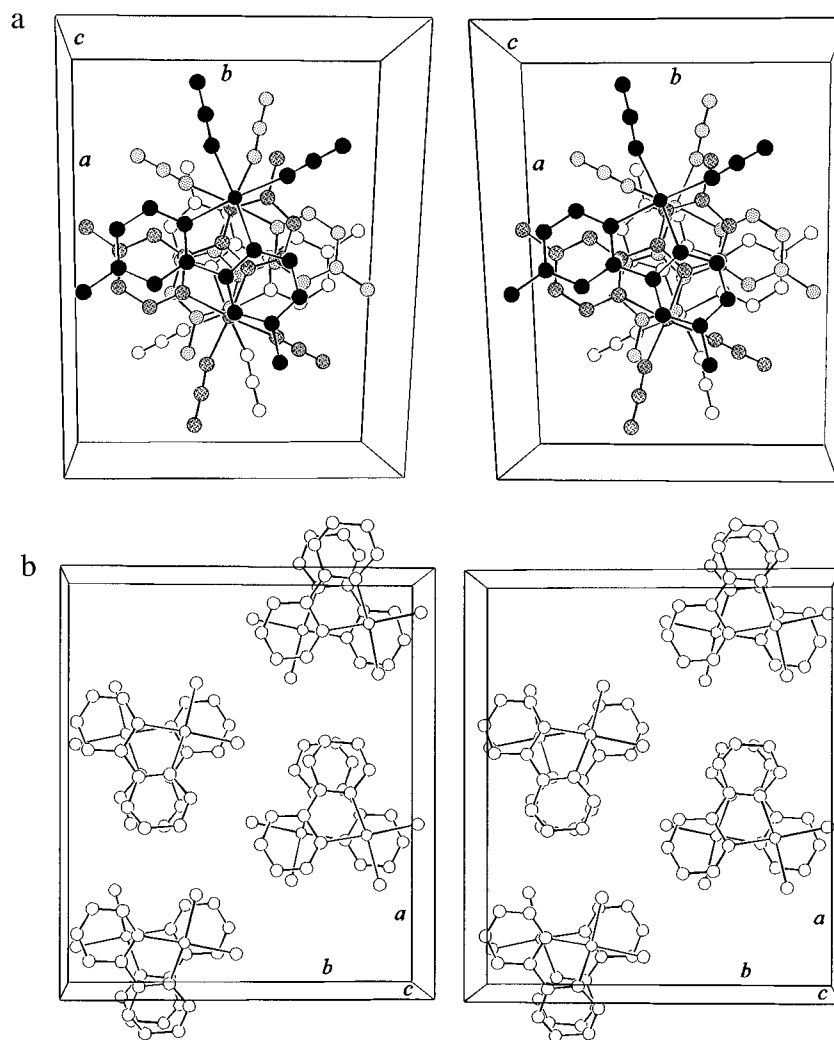
Figure 5. Stereoviews of crystal packing: (a) the yellow form of Pt(dmbpy)(NCO)$_2$ (**1b**) with four of the molecules in the unit cell shown; (b) the yellow form of Pt(bpy)Cl$_2$.[21] H atoms are omitted for clarity.

Table 4. Structural Properties of Linear-Chain Platinum Halides

compound	Pt⋯Pt (Å)	ref
[Pt(NH$_3$)$_4$][PtCl$_4$]	3.24	5
cis-Pt(NH$_3$)$_2$Cl$_2$	3.37, 3.41	44
Pt(en)Cl$_2$, orthorhombic form	3.38	45
Pt(en)Cl$_2$, triclinic form	3.42, 3.51	*b*
Pt(dada)Cl$_2$, polymorph I[a]	3.39	48
Pt(dada)Cl$_2$, polymorph II[a]	3.65	48
Pt(en)Br$_2$	3.50	46
Pt(amp)(CO)I[a]	3.50	*c*
Pt(1,2-benzoquinonedioxime)I$_2$	3.67, 3.71	47

[a] Key: amp = (2-aminomethyl)phenyl; dada = diaminodideoxyalditol. [b] Ellis, L. T.; Hambley, T. W. *Acta Crystallogr.* **1994**, *C50*, 1888. [c] Avshu, A.; O'Sullivan, R. D.; Parkins, A. W.; Alcock, N. W.; Countryman, R. M. *J. Chem. Soc., Dalton Trans.* **1983**, 1619.

3).[45] Decreased ligand-field strength also accounts for the slightly longer separation of 3.50 Å in Pt(en)Br$_2$,[46] as well as the 3.673(2) and 3.707(2) Å distances in Pt(1,2-benzoquino-nedioxime)I$_2$.[47] While the spacings in this series are also consistent with steric effects, it should be noted that the steric

congestion around Pt(dada)Cl$_2$ (dada = diaminodideoxyalditol) does not preclude stacking (Pt⋯Pt = 3.388(2) Å).[48]

The most compelling evidence for these electronic effects comes from comparison of the bpy complexes with their bpm analogues. These ligands have nearly the same shape and their packing requirements should be very similar. However, their electronic properties are substantially different, because bpm is both a better π-acceptor and a better σ-donor than bpy.[49] These differences are evident in the structures of compounds **2** and **3**, as well as those of **6** and **8**. The two Pt⋯Pt distances in Pt(bpm)Cl$_2$·0.5(nmp) (**3**) are 0.04 and 0.08 Å shorter than in Pt(bpy)Cl$_2$ (**2**); similarly, the Pt⋯Pt distance in Pt(bpm)(CN)$_2$· (dmf) (**8**)[9] is 0.06 Å shorter than in Pt(bpy)(CN)$_2$ (**6**) and 0.05– 0.06 Å shorter than in the other dicyano structures (**5**, **6**). This observation is consistent with ligand-induced enhancement of the Pt⋯Pt interactions between stacked complexes.[50] The molecular shape of Pt(bph)(CO)$_2$ (**10**) also is quite similar to that of compounds **6** and **8**; **10** has the shortest Pt⋯Pt distance of these three compounds, which is entirely consistent with the strong σ-donor properties of the bph ligand and the π-acceptor character of the carbonyl groups.

(44) Milburn, G. H. W.; Truter, M. R. *J. Chem. Soc. A* **1966**, 1609.
(45) Iball, J.; MacDougall, M.; Scrimgeour, S. *Acta Crystallogr.* **1975**, *B31*, 1672.
(46) Kroening, R. F.; Hunter, L. D.; Rush, R. M.; Clardy, J. C.; Martin, D. S. *J. Phys. Chem.* **1973**, *77*, 3077.
(47) Mégnamisi-Bélombé, M.; Endres, H. *Acta Crystallogr.* **1985**, *C41*, 513.

(48) Hanessian, S.; Gauthier, J.-Y.; Okamoto, K.; Beauchamp, A. L.; Theophanides, T. *Can. J. Chem.* **1993**, *71*, 880.
(49) Ernst, S. D.; Kaim, W. *Inorg. Chem.* **1989**, *28*, 1520.
(50) Alternatively, the incorporation of solvent into the structures of **3** and **8** may allow closer approach of the metal centers through more efficient packing.

Supporting Information Available: Tables giving complete crystallographic experimental details, distances and angles, positional parameters for all atoms, and anisotropic displacement parameters and ORTEP drawings (31 pages). Ordering information is given on any current masthead page.

IC961232V